CARBON 50 (2012) 1455–1464

Available at www.sciencedirect.com

SciVerse ScienceDirect

journal homepage: www.elsevier.com/locate/carbon

The electrical conductivity and electromagnetic interference shielding of injection molded multi-walled carbon nanotube/polystyrene composites

Mehdi Mahmoodi [a], *Mohammad Arjmand* [b], *Uttandaraman Sundararaj* [b], *Simon Park* [a,*]

[a] *Department of Mechanical and Manufacturing Engineering, University of Calgary, Calgary, AB, Canada T2N 1N4*
[b] *Department of Chemical and Petroleum Engineering, University of Calgary, Calgary, AB, Canada T2N 1N4*

ARTICLE INFO

Article history:
Received 6 August 2011
Accepted 5 November 2011
Available online 25 November 2011

ABSTRACT

Multi-walled carbon nanotube (MWCNT)/polystyrene (PS) composites were injection molded into a mold equipped with three different cavities. A high alignment of MWCNTs in PS was achieved by applying high shear force to the melt. The effects of gate and runner designs and processing conditions, i.e., mold temperature, melt temperature, injection/holding pressure and injection velocity, on the volume resistivity of the composites were investigated in both the thickness and in-flow directions. The experiments showed that volume resistivity could be varied up to 7 orders of magnitude by changing the processing conditions in the injection molded samples. The electromagnetic interference shielding effectiveness (EMI SE) of the molded composites was studied by considering the alignment of the MWCNTs. The EMI SE decreased with an increase in the alignment of the injection-molded MWCNTs in the PS matrix. This study shows that mold designs and processing conditions significantly influence the electrical conductivity and shielding behavior of injection molded CNT-filled composites.

1. Introduction

Carbon nanotubes (CNTs) are promising additives for thermoplastics, due to their superior mechanical, thermal, magnetic and electrical properties [1,2]. Due to the high electrical properties of CNT/polymer composites and their application in electrostatic discharge dissipation, electromagnetic interference (EMI) shielding, printable circuit writing and transparent conductive coatings, these materials have attracted great attention, both in academia and industry [3,4].

Many researchers have investigated the electrical properties of CNT and thermoplastic composites prepared with the melt mixing method [2,5], but only a small number of studies have chosen injection molding as the method of shaping the conductive polymer composites (CPCs) [6–8]. Injection molding is a common method to fabricate thermoplastic components. Compared to other manufacturing processes, such as compression molding, the injection molding method can produce CNT/polymer composites in a short production cycle and has the ability to produce complicated 3D parts, making it suitable for batch production of composites. Furthermore, a wide range of thermoplastic materials can be processed by this manufacturing procedure.

The shear flow in the injection molding process significantly influences the alignment of CNTs in the molded composites, and this can shift the percolation threshold to higher filler concentrations by decreasing the probability of fiber–fiber contact [6,8,9]. This can be a disadvantage when

* *Corresponding author:* Fax: +1 403 282 8406.
E-mail address: simon.park@ucalgary.ca (S. Park).
0008-6223/$ - see front matter
doi:10.1016/j.carbon.2011.11.004

high electrical conductivity is desired or can be an advantage when high alignment of CNTs is preferred in a particular direction.

The alignment of nanotubes in injection molded parts has been explored by several researchers. Abbasi et al. [8] performed a study on the alignment of the CNTs in polycarbonate using different processes and concluded that a high degree of CNT alignment and, consequently, a higher percolation threshold would be obtained by micro injection molding than with compression molding. Villmow et al. [6] investigated the impact of processing parameters on the electrical surface and volume resistivities of the injection molded parts and concluded that the melt temperature and injection velocity, as well as their interaction, have the highest impact on the volume resistivity of the samples. To best of our knowledge, no research study has been reported on the influence of mold designs on the electrical conductivity of the injection molded parts.

Similar to the conductivity of CNT-based composites, extensive amounts of research have been performed on their EMI shielding effectiveness (SE). Their high electrical conductivity along with their high aspect ratio have made CNTs an excellent option for manufacturing high-performance EMI shielding materials at low filler loading. Al-Saleh and Sundararaj [10] studied the shielding mechanism of multi-walled CNT (MWCNT)/polypropylene (PP) composites with different thicknesses and MWCNT concentrations. They found that, in MWCNT/PP composites, absorption is the main shielding mechanism followed by reflection.

In our previous study [11], we investigated the EMI SE of compression molded MWCNT/polycarbonate (PC) composites with different MWCNT concentrations. The results showed that both the material thickness and CNT loading can significantly affect the EMI SE of the CNT-filled composites. To study the EMI SE of nanotube-filled composites, previous researchers have mostly used compression molding and solution-based processing methods to shape the samples [10,12,13]. However, these processing methods cannot be properly applied in large-scale production of polymeric parts. For example, compared with the injection molding process, compression molding needs a longer processing time and is limited to producing simple, two-dimensional parts. Moreover, solution-based processing methods are time consuming; and there is also the possibility of damaging the surface properties of CNTs during the mixing procedure.

The focus of this paper is to investigate the effects of processing parameters and mold geometry on the electrical properties and EMI SE of injection molded MWCNT/PS composites. To achieve these goals, a mold equipped with three different cavities was designed and manufactured. The mold temperature, melt temperature, injection/holding pressure and injection velocity were considered as the variable parameters. The influences of the alignment of CNTs on the EMI shielding behavior of the molded CPCs were explored and discussed. This was further investigated by exploring the complex permittivity of the compression and injection molded samples.

The rest of this paper is organized as follows: Section 2 describes the materials, experimental setups, mold design and processing conditions. Section 3 deals with the results and discussions, which investigate the morphological characterization, volume resistivity, EMI SE and permittivity of the molded MWCNT/PS composites.

2. Materials and experimental setup

A masterbatch of 20 wt.% MWCNT/PS pellets (Hyperion Catalysis, MA, USA) was diluted to 5 wt.%. The MWCNTs were vapor grown and typically had an outer diameter of 10–15 nm wrapped around a hollow core of 5 nm in diameter [8]. The lengths ranged between 1 and 10 μm, while their density was approximately 1.75 g/cm^3. The pristine PS (Styron 610, Americas Styrenics LLC), with a melt flow index and density of 11 g/10 min (200 °C/5 kg) and 0.94–0.96 g/cm^3, respectively, was used to dilute the masterbatch. Before processing, all the materials were dried at 80 °C for at least 4 h. The masterbatch was diluted into 5 wt.% of MWCNT/PS using a co-rotating twin-screw extruder.

The experiments were conducted using a micro injection molding machine (Boy 12A) with a screw diameter of 18 mm and a length to diameter (L/D) ratio of 20. A series of experiments were conducted using a two-level, four-factor factorial design to investigate the impact of four process parameters, i.e., mold temperature (c_1), melt temperature (c_2), injection/holding pressure (c_3) and injection velocity (c_4), on the volume resistivity and EMI SE of the molded samples.

The set points were selected with the maximum possible interval, considering the limitations of the used micro injection molding machine and also the recommended processing conditions of pure PS. Constant holding and cooling times of 8 and 10 seconds, respectively were applied for all the experiments. It should be mentioned that the holding pressure was set the same as the injection pressure for all runs. The volume resistivity was measured both in the in-flow and thickness directions of the molded samples.

A mold equipped with three cavities was designed and manufactured on a 3-axis micro milling center (Kern Micro MC2522) using a WC 700 μm taper-end mill tool with a 2-degree taper angle and spindle speed of 100,000 rpm. The cavities were the same size with dimensions of $22.86 \times 10.16 \times 2.00$ mm, but were fed with different gates and runners.

Fig. 1(a) shows a schematic of the designed mold with the dimensions provided in Table 1. Cavity #1 was fed by a trapezoidal runner and an edge gate; Cavity #2 was fed by a trapezoidal runner and a fan gate; and, Cavity #3 was fed by a trapezoidal runner and an edge gate, but the position of the gate was located at the longer edge of the rectangular cavity. The runner and gate dimensions were balanced using Moldflow™ software for PS to ensure that all the cavities were filled at the same time. Fig. 1(b) shows a schematic of the filling step simulated using control volume finite element method software (Trademark of Moldflow software, Ver. 5), showing that all the cavities had the same filling time.

All the samples had the same cavity size, but the runner and gate shapes and positions differed from each other. A detailed description of the mold is given in the next section. Tables 2 and 3 show the experimental design and the set points of the molding parameters, respectively.

A compression molding machine (Carver, Wabash, IN) was used to make rectangular samples the same size as the

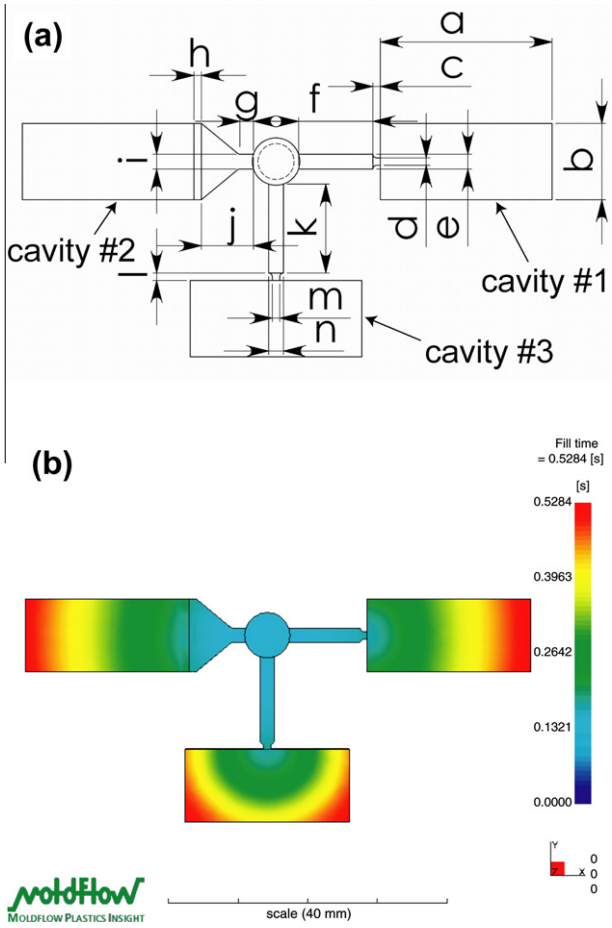

Fig. 1 – (a) A schematic view of the designed mold and (b) filling simulation of the cavities using Moldflow™ software.

injection molded samples, in order to compare their electrical conductivity with the conductivity of injection molded samples. The compression molding process was carried out for 5 min at 344.7 bar (5000 psi) and 200 °C.

Two different resistivity measurement setups were used to measure the volume resistivities of the compression and injection molded samples. A Loresta GP resistivity meter (MCP-T610 model, Mitsubishi Chemical Co., Japan) was utilized to measure the electrical volume resistivity of the samples with a volume resistivity less than 10^4 Ω cm, according to ASTM 257-75. Volume resistivities higher than 10^4 Ω cm were measured with a Keithley 6517A electrometer connected to a Keithley test fixture (Keithley Instruments, USA). The applied voltage to measure resistivity was 10 V.

The EMI SE and permittivity measurements were performed in the X-band frequency range (8.2–12.4 GHz) using an Agilent vector network analyzer (VNA) (Model 8719 ES). The rectangular sample (22.86 × 10.16 × 2.00 mm) was placed between two X-band waveguide parts, which were connected to separate ports of the VNA. The samples to be tested were slightly bigger than X-band waveguide windows. The VNA sent a signal down the waveguide upon the sandwiched sample and the power of the incident, reflected and transmitted waves were measured by three wave detectors to calculate the SE by reflection and absorption.

Table 1 – Dimensions of the designed 3-cavity mold.

Parameter	Value (mm)
a	22.86
b	10.16
c, *d*, *h*, *l*, *m*	1.00
e, *i*, *n*	2.00
f	10.00
g	1.84
j	7.00
k	12.00

Table 2 – Experimental design showing the two-level, four factor factorial design. The factors are c_1 – mold temperature, c_2 – melt temperature, c_3 – injection/holding pressure, and c_4 – injection velocity.

Exp. #	Factors			
	c_1 (°C)	c_2 (°C)	c_3 (bar)	c_4 (mm/s)
1	–	–	–	–
2	–	–	–	+
3	–	–	+	+
4	–	–	+	–
5	–	+	–	–
6	–	+	–	+
7	–	+	+	+
8	–	+	+	–
9	+	+	–	–
10	+	+	–	+
11	+	+	+	+
12	+	+	+	–
13	+	–	+	–
14	+	–	+	+
15	+	–	–	+
16	+	–	–	–

Table 3 – Levels (set points) of the experiments.

Level	Factors			
	c_1 (°C)	c_2 (°C)	c_3 (bar)	c_4 (mm/s)
+	60	240	100	240
–	25	215	60	24

3. Results and discussion

Transmission electron microscopy (TEM) was applied to the samples to characterize the molded composites. The variations in the thickness and in-flow volume resistivities of the molded CPCs by changing the processing conditions and geometry of the mold are discussed. Also, the EMI SE and permittivity of the injection molded composites with different electrical conductivity are explored.

3.1. *Morphological characterization*

The electrical conduction pathways within the polymer matrix are obtained when a network of CNTs is created, which is

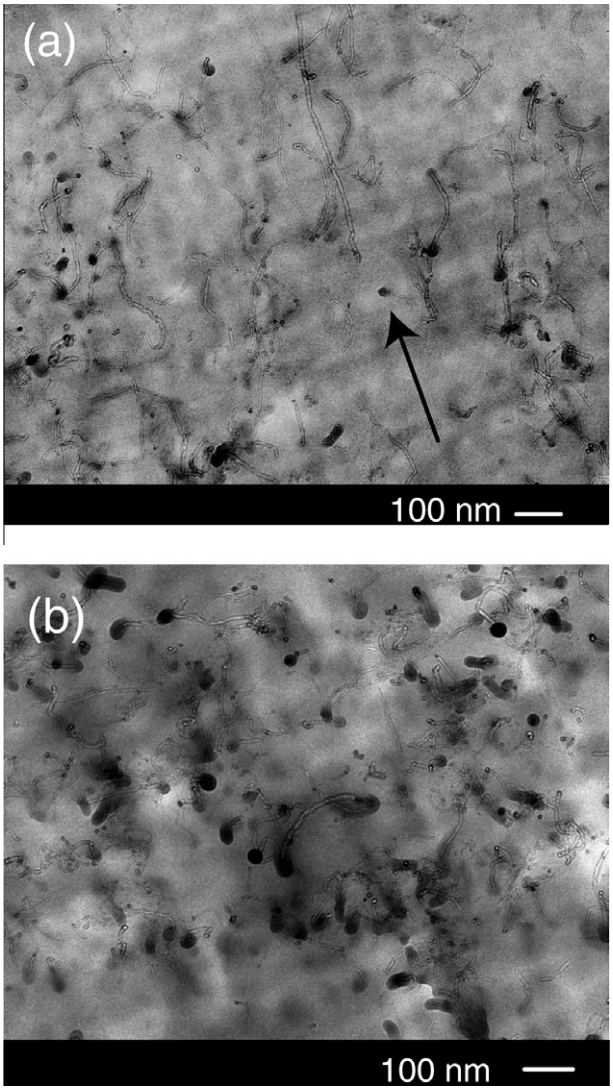

Fig. 2 – TEM images from (a) parallel to the flow from injection molded sample #14 and (b) compression molded sample.

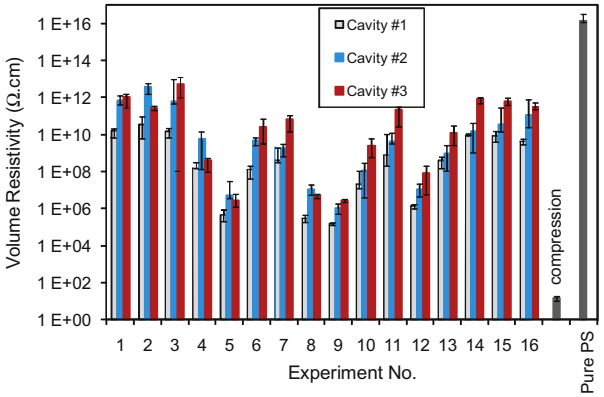

Fig. 3 – Volume resistivities of the molded parts in the thickness direction.

known as the percolation threshold. As explained previously, the alignment of CNTs can significantly influence the percolation threshold by decreasing the probability of CNT–CNT contact. To examine the alignment and distribution of CNTs within the PS matrix, TEM scanning (Hitachi H-7650) of the samples was conducted. The samples for TEM scanning were ultra-microtomed (70 nm in thickness) using a glass knife at room temperature.

Fig. 2(a) shows a TEM image taken from a part molded in Cavity #1 parallel to the flow direction. A good dispersion of MWCNTs can be observed within the PS matrix, proving the effective mixing of the twin-screw extruder. The flow direction is also shown in this picture. As can be seen, the CNTs were more aligned in the in-flow direction along their length axis, due to the effect of the shear flow in injection molding. However, considering the entanglement of the CNTs and their curved structure, some of them remained transverse to the in-flow direction. Fig. 2(b) shows a TEM image from compression molded samples. As can be seen in this image, no preferable alignment can be observed in this image.

3.2. *Electrical resistivity*

The electrical resistivities of the molded samples in the thickness direction were measured and are given in Fig. 3. This figure shows the resistivity of the MWCNT/PS composites for three different cavities and compares them with the value obtained from compression molding. The results show a decrease of about 10 orders of magnitude in volume resistivity by adding 5 wt.% MWCNT, compared with pure PS. Interestingly, depending on the runner and gate type, position and processing conditions, differences in the volume resistivity of up to 7 orders of magnitude can be observed in the thickness direction of the composites.

In Fig. 3, the highest resistivity of the samples can be observed for the first three and last three experiments, where c_2 (melt temperature) was minimal. This result can be explained by the fact that decreasing the melt temperature can increase the melt viscosity and, consequently, the shear force exerted to the melt, leading to an increase in CNT alignment. This can decrease the probability of CNT–CNT contact and, accordingly, decrease the chance of conducting electrons through the CNT network.

The lowest amount of volume resistivity (i.e., the highest amount of electrical conductivity) can be seen in experiments 5, 8, 9 and 12. From Table 2, in these experiments, c_2 (melt temperature) had the highest values, and c_4 (injection velocity) had the lowest values. This decrease in volume resistivity resulted from the formation of the conductive network in the polymer structure. The low shear force applied to the melt, due to the decrease in the shear rate and viscosity that were induced by the low injection velocity and high melt temperature, respectively, helped the formation of a percolated network of CNTs.

Among the cavities, Cavity #1, which was equipped with an edge gate, showed the lowest volume resistivity compared with the other two cavities. It is worthwhile mentioning that, in a comparison between Cavities #1 and #2 (with edge and fan gates, respectively), the volume resistivity of the parts molded with the edge gate cavity (#1) was lower than that of the fan gate cavity (#2).

The electrical resistivities of the samples along the in-flow direction were measured and are shown in Fig. 4. To measure

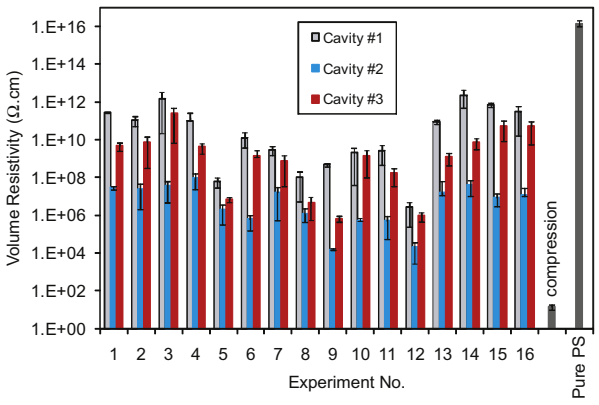

Fig. 4 – Volume resistivity of the molded composites parallel to the in-flow direction.

the volume resistivity parallel to the in-flow direction, samples of 2.00 mm thickness were cut from the near gate location. It should be mentioned that the samples from Cavity #3 were cut parallel to their longer side for measuring their volume resistivity. As with the resistivity of the samples in the thickness direction, a difference of up to 7 orders of magnitude in volume resistivity parallel to the in-flow direction was observable. Among the injection molded samples, the highest volume resistivity was observed for processing condition (PC) #14, Cavity #1 (2.29×10^{12}); and, the lowest volume resistivity was observed for PC #9, Cavity #2 (1.58×10^{4}).

An interesting trend was observed in the in-flow resistivity of the samples. Parts molded with Cavity #1 showed the highest volume resistivity among the samples. In other words, the highest alignment parallel to the in-flow direction was obtained with Cavity #1. It is worthwhile mentioning that Cavity #1 was the one with the trapezoidal runner and the edge gate located at the smaller side of the rectangular cavity (Fig. 1(a)). Samples molded with Cavity #2 (trapezoidal runner and fan gate) showed the lowest electrical resistivity, because a conductive network of CNTs in the in-flow direction could be better formed in Cavity #2. The resistivities of the samples molded with Cavity #3 were between those of Cavities #1 and #2.

Another interesting observation can be made with a comparison between the resistivities in the flow and thickness directions. Cavity #1 showed the highest volume resistivity among the cavities in the in-flow direction (Fig. 4), while the lowest amount of volume resistivity was observed for Cavity #1 in the thickness direction (Fig. 3). So it can be concluded that among the cavities used in this study, the edge gate cavity resulted the highest volume resistivity in the in-flow direction and the lowest volume resistivity in the thickness direction. Another interesting phenomenon is the volume resistivities of the molded samples with the fan gate cavity (Cavity #2) in the in-flow and thickness direction. For this cavity, volume resistivities in the in-flow direction are noticeably less than in the thickness direction which can be interpreted that less CNT–CNT contacts have formed in the thickness direction compared to the in-flow.

Similar to the resistivity in the thickness direction (Fig. 3), the lowest volume resistivity of the samples in the in-flow direction can be observed in experiments 5, 8, 9 and 12 (Fig. 4). These four experiments had samples molded at a high melt temperature and a low injection speed, again indicating that these two parameters have the greatest influence on the volume resistivity of the molded composites.

To analyze the data of the in-flow resistivity, statistical software (Trademark of Minitab software, ver. 14) was used to find the importance of each factor and their combinations. The effects of the main factors on the volume resistivity of the composites molded with Cavity #1 are plotted in Fig. 5(a). This plot shows the effect of each independent variable (c_1–c_4) on the volume resistivity of the samples. As can be seen in Fig. 5(a), c_2 (melt temperature) and c_4 (injection speed) show the greatest impact on the volume resistivity of the samples. However, as was previously mentioned, their significant effects can be explained by their influence on changing the shear rate exerted to the melt and CNTs.

To better understand the interaction of the factors on the volume resistivity of the samples, interaction plots were produced and are shown in Fig. 5(b). In this figure, the interaction plot shows the mean volume resistivity of two factors at all possible conditions. Parallel lines in an interaction plot mean that there was no interaction between the two corresponding factors; and, when the lines diverge, it means that there was an interaction between the factors. The greater the distance, the higher was the interaction that existed between the parameters. Based on Fig. 5(b), the interactions of c_2 and c_4 (shown as c_{24} in this paper) and of c_3 (injection/holding pressure) and c_4 (c_{34}) had the greatest impact on the volume resistivity of the composites. For c_{24}, when c_2 was at a low level (215 °C), an increase in the volume resistivity could be observed when c_4 changed from level −1 to level +1.

The effect of injection velocity (c_4) seemed to be low when the melt temperature (c_2) was set at a high value (240 °C); whereas, at a low melt temperature (215 °C), the effect of the injection velocity was more significant, due to the considerable change in increasing the shear rate exerted to the melt. For c_{34}, an increase in volume resistivity could also be observed when c_3 was set on its high level and c_4 was changed from −1 to +1 levels. Polymeric chains tend to keep their orientation in the in-flow direction at a higher injection/holding pressure. In other words, a higher holding pressure can reduce melt relaxation, so that more of the fill-induced orientation of the chains and CNTs can be retained. Consequently, at a higher injection/holding pressure (c_3), CNTs are more aligned in the in-flow direction, and a higher volume resistivity can be achieved. The interaction of some parameters, such as c_{12}, c_{13} and c_{14}, did not have a significant effect on the volume resistivity of the molded samples.

As a result, it can be concluded that a high melt temperature and low injection velocity can help decrease the degree of CNT alignment and thus increase the electrical conductivity in injection molded components. Moreover, using a fan gate in an injection mold contributes to achieving a higher electrical conductivity compared to edge gate.

3.3. *EMI shielding effectiveness (SE)*

Electromagnetic interference (EMI) is defined as the effect of undesirable signals on electronic systems, make their

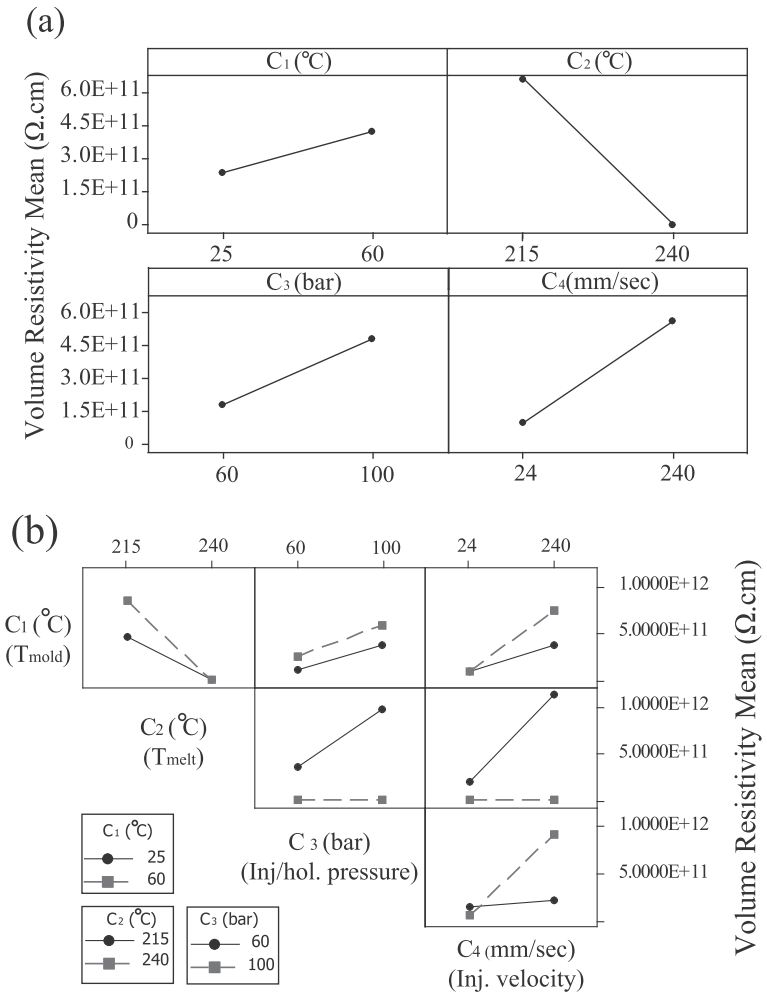

Fig. 5 – (a) Minitab main effect plot of the volume resistivity mean of the molded samples with Cavity #1 and (b) interaction plot for volume resistivity of the composites.

functionality difficult or impossible. These unwanted electromagnetic (EM) waves can be blocked using a conductive shield. Currently, metal-coated or -plated polymers are widely used as EMI shields, but these materials have some drawbacks, such as delamination and difficulty in recycling [14,15]. To minimize the process cost and increase the effectiveness, CNTs can be embedded into a polymer matrix to make a conductive composite and interact with the incident EM wave.

To attain composites with high EMI SE and low filler amount, understanding the shielding mechanism of conductive materials is important. The mechanism of EMI shielding for a conductive monolithic material is described in the following paragraphs, and the results obtained from the EMI tests are then explored.

When an EM wave hits a shield, the electrons and other charged particles inside the shield respond to the incident wave by creating a scattered field or induced field. The induced field changes the total field inside the shield, which affects the charge motion [16]. Three different mechanisms contribute to the shielding of an incident EM wave, namely: reflection, absorption and multiple-reflection [16,17].

When the shield is sufficiently distant from the source of the field (in the far field region), the wave can be considered as a plane wave, and the electric field and magnetic field are perpendicular to each other [16,17]. When an incident wave strikes the shield, a portion of wave is reflected back via interaction with surface charges. Mobile charge carriers (electrons and holes) interact with the EM wave in reflection [18]. Therefore, the material used as the EMI shield tends to be conductive, due to mobile charge carriers. However, this does not mean that conductivity is the absolute criterion for EMI shielding, as conduction needs connectivity between the fillers; whereas, this is not necessary for EMI shielding. However, EMI SE is improved by increasing the conductivity, as confirmed by previous research works [10,11].

Another mechanism of shielding in conductive materials is absorption. A portion of the incident electric field that penetrates inside the shield is attenuated through this mechanism. The amplitude of the penetrated wave is attenuated according to $e^{-\alpha z}$, where α is the attenuation constant of the shield and z is the distance from the shield's surface. For good conductors, the attenuation constant is related to the skin depth of the material (δ) according to $\alpha = \delta^{-1}$, where $\delta = 1/\sqrt{\pi f \mu \sigma}$, f is the frequency (Hz), and μ and σ are magnetic permeability and conductivity of the shield, respectively [16,17]. The skin depth is the distance inside the shield where

the wave strength decreases to e^{-1} ($e = 2.718$) of its incident value. To have significant absorption, the material needs to have electric and/or magnetic dipoles and a high amount of mobile charge carriers to interact with the EM fields [16,18,19].

The last mechanism of EMI shielding is multiple-reflection, which refers to the internal reflection inside the shield. Multiple-reflections are said to decrease the overall SE when the shield thickness is less than shield's skin depth and can be neglected when the shield is thicker than the skin depth or when shielding by absorption is more than 10 dB [10,13,16,17,20].

Shielding by reflection (SE_R), absorption (SE_A) and multiple-reflection (SE_{MR}) contribute to the overall SE according to the following equation [16]:

$$SE = SE_R + SE_A + SE_{MR} = 10 \log\left(\frac{P_{in}}{P_{out}}\right) \quad (1)$$

where P_{in} is the incident power and P_{out} is the transmitted power.

To investigate the effect of the alignment of CNTs and, consequently, the composite's electrical conductivity on EMI SE, molded samples with different electrical conductivity were selected. For this purpose, three different injection molding processing conditions (PCs #4, 12 and 16) were selected. These processing conditions were selected, as they had exhibited medium, high and low average electrical conductivity in the previous experiments. The average electrical conductivity in the EMI SE section of this paper is defined as the mean of the thickness and in-flow electrical conductivities for each PC. Table 4 shows the average electrical conductivity (S/cm) and the measured EMI SE (dB) of the selected samples.

To obtain a better insight into the correlation between the EMI SE and the electrical conductivity/resistivity data, the EMI SEs (dB) of the samples shown in Table 4 were plotted versus the electrical resistivities of the specimens (Ω cm), as shown in Fig. 6. The EMI SE of the pure PS was almost zero, as the electrical conductivity of this material is negligible. A decrease in volume resistivity or an increase in electrical conductivity, σ, led to an increase in the EMI SE of the molded samples. It should be noted that all the samples had the same MWCNT concentrations (5 wt.%); therefore, they had same amount of mobile charge carriers. Hence, there should be other factors that contribute to an increase of the EMI SE of the samples with higher electrical conductivities. To clarify this, the absorption and reflection behavior of the molded CPCs are separately explored and presented in the following paragraphs.

For conductive monolithic materials, following equations are suggested to determine reflection, absorption and multiple-reflection, respectively [10,16,17,21]:

$$SE_R = 168 + 10 \cdot \log_{10}\left(\frac{\sigma_r}{\mu_r \cdot f}\right) \quad (2)$$

$$SE_A = 131 \cdot 4d\sqrt{f\mu_r\sigma_r} \quad (3)$$

$$SE_{MR} = 20 \cdot \log\left|1 - e^{-2\frac{d}{\delta}} \cdot e^{-j2\frac{d}{\delta}}\right| \quad (4)$$

where σ_r is the electrical conductivity of the shield relative to the copper, μ_r is the magnetic permeability of the shield relative to the free space ($\mu_0 = 4\pi \times 10^{-7}$ H/m), f is the frequency of EM wave, d is the shield thickness and δ is the shield's skin depth. However, the above equations are developed for conductive monolithic materials and applying these equations to CPCs with different filler alignments does not sufficiently lead to proper answers. It is evident that absorption shows a direct relation with conductivity and permeability; while reflection increases with increase in conductivity and decreases with increase in permeability.

Fig. 7 shows the SE by reflection (SE_R) and absorption (SE_A) of the CPCs versus the logarithm of their volume resistivity. Absorption tended to decrease by increasing the alignment of the MWCNT particles; whereas, interestingly, reflection showed a reverse trend. For the compression molded sample, which had the highest electrical conductivity, absorption was significantly higher than reflection. An increase in the absorption of the CPCs with higher random alignment can be attributed to the increase in real permittivity due to the higher polarization, imaginary permittivity and also the increase in the electrical conductivity of the molded CPCs. This is further explained in next section, where permittivity data are presented.

By decreasing the electrical conductivity, reflection showed greater contribution to shielding than absorption. One reason for this could be the higher alignment of

Table 4 – Average volume resistivity (Ω·cm), conductivity (S/cm), and corresponding EMI SE (dB) of the molded samples (PCs #12, 4 and 16) for different cavities.

		Average volume resistivity (Ω·cm)	Average electrical conductivity (S/cm)	EMI SE (dB)
PC #12	Cavity #1	2×10^6	5×10^{-7}	11.46
	Cavity #2	5.1×10^6	1.96×10^{-7}	11.08
	Cavity #3	4×10^7	2.5×10^{-8}	10.32
PC #4	Cavity #1	9×10^9	1.04×10^{-10}	8.9
	Cavity #2	2.73×10^9	3.66×10^{-10}	9.15
	Cavity #3	2.24×10^9	4.46×10^{-10}	9.2
PC #16	Cavity #1	1.59×10^{11}	6.29×10^{-12}	8.04
	Cavity #2	5.35×10^{10}	1.87×10^{-11}	8.86
	Cavity #3	2.05×10^{11}	4.88×10^{-12}	8.05
Compression molding		14	0.071	17.2

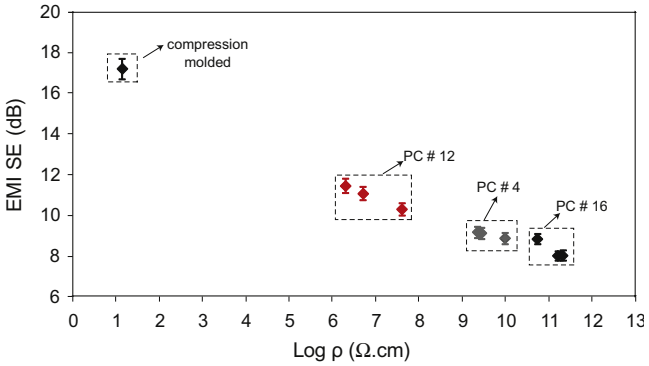

Fig. 6 – EMI SE (dB) of the injection and compression molded composites vs. volume resistivity (Ω·cm).

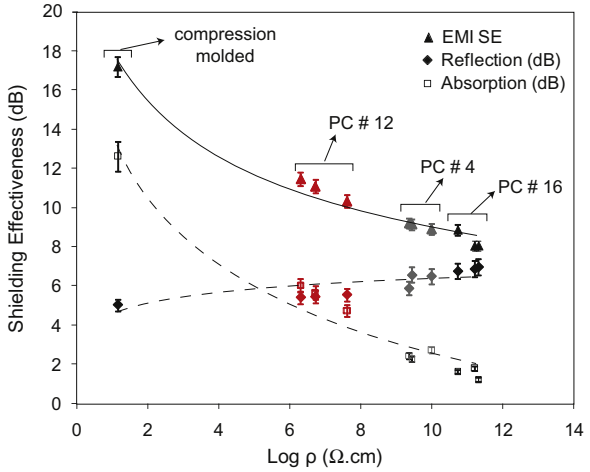

Fig. 7 – Reflection and absorption of the compression and injection molded samples (PCs #4, 12 and 16).

MWCNTs on the surface of the injection molded samples. The alignment of CNTs on the surface of the molded CPCs was much higher than that in the core, especially when a high shear force had been applied to the melt. This has also been shown by Villmow et al. [6]. Therefore, for the samples with a higher degree of alignment (PCs #4 and 16), more MWCNTs were expected to be exposed on the surface, which led to a higher amount of interacting charge carriers on the surface. This may have resulted in a greater amount of reflection in the samples with higher CNT alignment.

3.4. *Complex permittivity analysis*

To further elucidate the absorption behavior of the CNT-filled composites, their permittivity needed investigation. When an electromagnetic wave strikes a conductive surface, two different electric currents induced inside the material, namely the conduction and displacement currents [22]. Conduction current is assumed to be due to the free electrons and to provide electric loss (imaginary permittivity) inside the material. The displacement current arises from the localized charges, i.e., polarization (real permittivity) [23].

Complex permittivity is defined as $\varepsilon^* = \varepsilon' - j\varepsilon''$, where ε' is the real permittivity of the material. Real permittivity is mainly affected by the amount of the polarization inside the material. ε'' is defined as the imaginary permittivity of the material and is equal to $\sigma/\omega\varepsilon_0$ for conductive monolithic materials, where $\varepsilon_0 = 8.854 \times 10^{-12}$ F/m is the permittivity of the free space and ω is the angular frequency of the applied field. Fig. 8 shows the experimental values of the real and imaginary permittivities of the compression and injection molded samples for selected processing conditions (PCs #4, 12 and 16), by using the Nicholson–Ross–Weir method [24].

As Fig. 8 shows, both the real and imaginary permittivities increased with increases in electrical conductivity (decreases in electrical resistivity). To clarify this behavior, we can consider the MWCNT/PS composite as a circuit with a capacitor (MWCNT/PS) in parallel to a resistor (MWCNT). Since the CNT alignment in samples with higher volume resistivity was higher, the gap distance between the MWCNTs in these processing conditions (PCs #4 and 16) was higher than the others. Therefore, the chance of electron transfer from one MWCNT to the other ones in its neighbor decreased.

For compression molded samples and injection molded samples molded with PC #12, due to the more random distribution of CNTs, the gap distance between neighbor MWCNTs was smaller; therefore, electrons had a higher chance of transfer. It is worth mentioning that, in narrow insulating gaps between CNTs, a high electric field is created, the strength of which is higher than the macroscopic voltage by a factor of M, which is equal to the average size of the conducting fillers to the average junction width [25,26]. This high-strength field provides sufficient energy for the electrons to transfer from the insulative gaps in the form of conduction current. Therefore, a higher amount of imaginary permittivity can be observed for compression molded samples and PC #12 injection molded specimens.

As Fig. 8(a) shows, real permittivity, which influences the polarization of the samples, tended to increase by increasing the electrical conductivity. Depending on the cavity type, processing condition and thus conductivity, the real permittivity varied from 11 to 16 (F/m) for the compression and injection molded MWCNT/PS composites. When an electrical field strikes a CPC, the localized charges, i.e., electrons and protons, tend to redistribute themselves, which is known as polarization. Interfacial polarization is the most reported type of polarization mentioned in CPCs. However, because of the dielectric relaxation, this type of polarization has low influence at high frequencies (X-band frequency range). It is believed that high real permittivity of CNT-filled polymer composites at high frequencies is due to the CNT and polymer polarization [27,28].

Increasing the real permittivity of the composites by decreasing the volume resistivity can be attributed to the decrease in the gap distance between the CNT particles in the PS matrix and the increase in the electric field between the CNTs, which led to an increase in electronic polarization of the polymer matrix. For compression molded samples, the random distribution of CNTs helped to increase the amount of electronic polarization and, consequently, the real permittivity. High real permittivity contributes to increasing the shielding of an EM wave by the absorption mechanism.

It can, therefore, be concluded that, if high EMI SE is desired in injection molded CNT-filled composites, the mold

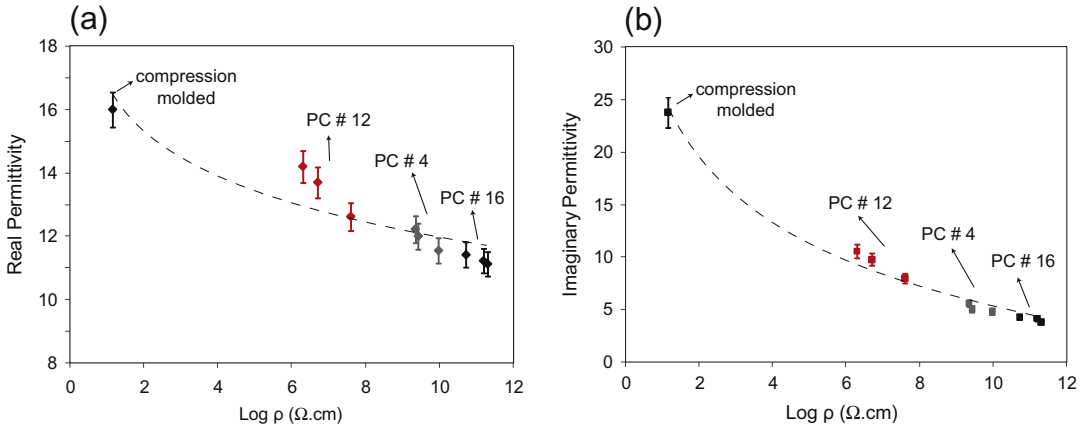

Fig. 8 – (a) Real and (b) imaginary permittivities of the compression and injection molded CPCs (PCs #4, 12 and 16).

design and process conditions should be properly adjusted to obtain a random distribution of CNTs inside the thermoplastic matrix. As our experiments showed, the random distribution of MWCNTs in PS increased the electrical conductivity of the CPCs and improved the EMI SE and both the real and imaginary permittivities of the molded specimens.

4. Conclusions

The volume resistivity and EMI SE of injection molded MWCNT/PS composites molded in three different cavities were investigated. The cavities were the same in size, but fed with different runners and gate designs in the injection molding process. The effects of the processing conditions on the electrical conductivity of the molded samples were examined using a two-level, four-factor factorial design. The results show that a higher electrical conductivity in injection molded parts can be obtained by using a high melt temperature and a low injection speed. It was also shown that using an edge gate led to higher volume resistivity in the in-flow direction and lower volume resistivity in the thickness direction, compared to when a fan gate was utilized.

The EMI SE behaviors of the molded samples with different electrical conductivity were measured and compared with each other. The results show that processing conditions in injection molding played a significant role in the shielding properties of molded CPCs. The EMI SE of the samples tended to increase by decreasing the degree of MWCNT alignment. The contributions of the reflection and absorption in the EMI shielding behavior of the samples were discussed. The experiments showed that reflection tended to increase by increasing the degree of alignment of the CNT on the shield's surface, while absorption exhibited a reverse trend. Specimens with randomly aligned MWCNTs showed higher real and imaginary permittivities, resulting into higher absorption of EM waves.

Acknowledgements

The authors would like to acknowledge Dr. Tieqi Li and Ms. Jeri-Lynn Bellamy of Nova Chemicals®, Calgary, AB, Canada for assistance with the polymer blending. The authors also would acknowledge Americas Styrenics LLC for donating the polystyrene material and Dr. Michal Okoniewski and Mr. Thomas Apperley from the Department of Electrical and Computer Engineering, University of Calgary, for their assistance in measuring the EMI SE of the samples.

REFERENCES

[1] Koerner H, Price G, Pearce NA, Alexander M, Vaia RA. Remotely actuated polymer nanocomposites—stress-recovery of carbon-nanotube-filled thermoplastic elastomers. Nat Mater 2004;3(2):115–20.
[2] Bauhofer W, Kovacs JZ. A review and analysis of electrical percolation in carbon nanotube polymer composites. Compos Sci Technol 2009;69(10):1486–98.
[3] Lellinger D, Xu D, Ohneiser A, Skipa T, Alig I. Influence of the injection moulding conditions on the in-line measured electrical conductivity of polymer–carbon nanotube composites. Phys Status Solidi B 2008;245(10):2268–71.
[4] Xie XL, Mai YW, Zhou XP. Dispersion and alignment of carbon nanotubes in polymer matrix: a review. Mater Sci Eng 2005;49(4):89–112.
[5] Ounaies Z, Park C, Wise KE, Siochi EJ, Harrison JS. Electrical properties of single wall carbon nanotube reinforced polyimide composites. Compos Sci Technol 2003;63(11):1637–46.
[6] Villmow T, Pegel S, Potschke P, Wagenknecht U. Influence of injection molding parameters on the electrical resistivity of polycarbonate filled with multi-walled carbon nanotubes. Compos Sci Technol 2008;68(3–4):777–89.
[7] Chandra A, Kramschuster AJ, Hu X, Turng LS. Effect of injection molding parameters on the electrical conductivity of polycarbonate/carbon nanotube nanocomposites. SPE-ANTEC Tech; 2007. p. 2184–8.
[8] Abbasi S, Carreau PJ, Derdouri A. Flow induced orientation of multiwalled carbon nanotubes in polycarbonate nanocomposites: rheology, conductivity and mechanical properties. Polymer 2010;51(4):922–35.
[9] Weber M, Kamal MR. Estimation of the volume resistivity of electrically conductive composites. Polym Compos 1997;18(6):711–25.
[10] Al-Saleh MH, Sundararaj U. Electromagnetic interference shielding mechanisms of CNT/polymer composites. Carbon 2009;47(7):1738–46.
[11] Arjmand M, Mahmoodi M, Gelves GA, Park S, Sundararaj U. Electrical and electromagnetic interference shielding

properties of flow-induced oriented carbon nanotubes in polycarbonate. Carbon 2011;49(11):3430–40.
[12] Li N, Huang Y, Du F, He X, Lin X, Gao H, et al. Electromagnetic interference (EMI) shielding of single-walled carbon nanotube epoxy composites. Nano Lett 2006;6(6): 1141–5.
[13] Zhang CS, Ni QQ, Fu SY, Kurashiki K. Electromagnetic interference shielding effect of nanocomposites with carbon nanotube and shape memory polymer. Compos Sci Technol 2007;67(14):2973–80.
[14] Huang JC. EMI shielding plastics – a review. Adv Polym Technol 1995;14(2):137–50.
[15] Bagwell RM, McManaman JM, Wetherhold RC. Short shaped copper fibers in an epoxy matrix: their role in a multifunctional composite. Compos Sci Technol 2006; 66(3–4):522–30.
[16] Kaiser KL. Electromagnetic shielding. Boca Raton, FL: CRC Press; 2006. p. 1–52.
[17] Paul CR. Introduction to electromagnetic compatibility. 2nd ed. New Jersey: John Wiley and Sons; 2006. p. 713–52.
[18] Chung DDL. Composite materials: functional materials for modern technologies. New York: Springer; 2003. p. 91–9.
[19] Schulz RB, Plantz VC, Brush DR. Shielding theory and practice. Electromagnetic compatibility. IEEE Trans 1998;30(3):187–201.
[20] Das NC, Maiti S. Electromagnetic interference shielding of carbon nanotube/ethylene vinyl acetate composites. Mater Sci 2008;43(6):1920–5.
[21] Li Y, Chen C, Zhang S, Ni Y, Huang J. Electrical conductivity and electromagnetic interference shielding characteristics of multiwalled carbon nanotube filled polyacrylate composite films. Appl Surf Sci 2008;254(18):5566–71.
[22] Fenske K, Misra D. Dielectric materials at microwave frequencies. Appl Microw Wireless 2000;12(12):92–100.
[23] Watts PCP, Hsu WK, Randall DP, Kroto HW, Walton DRM. Non-linear current–voltage characteristics of electrically conducting carbon nanotube–polystyrene composites. Phys Chem Chem Phys 2002;4(22):5655–62.
[24] Weir WB. Automatic measurement of complex dielectric constant and permeability at microwave frequencies. Proc IEEE 1974;62(1):33–6.
[25] Sichel EK, Gittleman JI, Sheng P. Transport properties of the composite material carbon-poly(vinyl chloride). Phys Rev B 1978;18(10):5712–6.
[26] Chekanov Y, Ohnogi R, Asai S, Sumita M. Electrical properties of epoxy resin filled with carbon fibers. J Mater Sci 1999;34(22):5589–92.
[27] Jiang MJ, Dang ZM, Bozlar M, Miomandre, Bai J. Broad-frequency dielectric behaviors in multiwalled carbon nanotube/rubber nanocomposites. J Appl Phys 2009;106(8):084902–6.
[28] Yuan JK, Yao SH, Dang ZM, Sylvestre A, Genestoux M, Bai J. Giant dielectric permittivity nanocomposites: realizing true potential of pristine carbon nanotubes in polyvinylidene fluoride matrix through an enhanced interfacial interaction. J Phys Chem 2011;115(13):5515–21.